Micromechanics-based model for trends in toughness of ductile metals

T. Pardoen[1] and J.W. Hutchinson[2]

[1]Département des Sciences des Matériaux et des Procédés, Université catholique de Louvain, PCIM, Place Sainte Barbe 2, B-1348 Louvain-la-Neuve, Belgium
[2]Division of Engineering and Applied Sciences, Harvard University, Cambridge, MA 02138, U.S.

Abstract: *A generic study of the relationship between fracture toughness and microstructure of ductile metals has been performed using a continuum damage model in a 2D small scale yielding finite element setting. The damage model is an enhanced Gurson model incorporating void shape effects and a micromechanical law for void coalescence. Emphasis is placed on cracking initiation. The results agree very well with recent calculations by Tvergaard and Hutchinson based on a finite element analysis which explicitly incorporates a row of voids in the discretization. The effect of the flow properties and of the void shape on the fracture toughness is discussed. Transition between a void by void growth and a multiple void interaction is analysed. The paper also addresses the difference between the fracture toughness at true cracking initiation and the fracture toughness defined in an engineering sense, i.e. after a given amount of crack propagation.*

INTRODUCTION

In the context of material science, the fracture toughness at cracking initiation is considered as the relevant parameter for indexing the fracture resistance of materials. The J integral at cracking initiation, J_{Ic}, is employed to characterize the toughness of ductile alloys that exhibit significant amount of crack tip plasticity. In general, J is measured experimentally as a function of the crack extension, i.e. the so-called " J_R-curve" method. The full J_R-curve obtained on laboratory specimens provides three important quantities: (1) the initiation toughness J_{Ic}, defined in an engineering sense, i.e. for a predetermined amount of crack growth, or, if it can be detected, at the physical event of cracking initiation; (2) an average tearing resistance dJ/da; and (3), when sufficient crack growth is allowed and sufficiently large specimens are used, the steady state fracture toughness, J_{ss}. In real specimen configuration, the intrinsic character of the J_R curve is, at best, limited to very small amount of crack extension. This paper addresses the material science point of view by studying the crack initiation toughness of ductile metal alloys failing by plastic void growth and the relationship with the microstructure. Of course, several aspects will be directly relevant for the "structural point of view" where emphasis is placed on integrity assessment rather than on the determination of material property.

Fig. 1 depicts the model envisioned for the cracking of ductile metal failing by a void growth mechanism. The initial geometry is a pre-crack of opening δ_0 in an ideal material having regularly distributed voids with spacing X_0 and radius R_0 in the crack plane. The flow properties of the material are characterized by the ratio of the

Young's modulus divided by the yield stress, E/σ_0, the Poisson ratio, ν, and a strain hardening exponent n. The dimensionless microstructural parameters are $\chi_0 = X_0/R_0$, $W_0 = R_{z0}/R_0$, and $\lambda_0 = Z_0/X_0$. The porosity f_0 is univocally related to these variables.

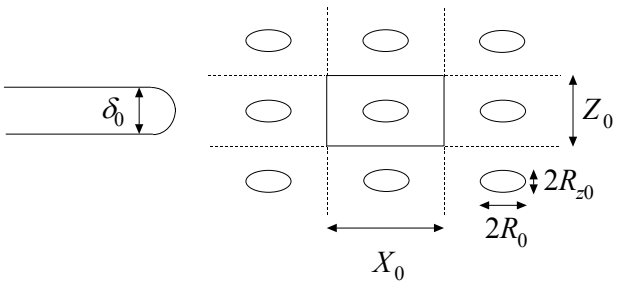

Figure 1: initial geometry of a precrack in an ideal material with regularly distributed spheroidal inclusions.

Except for the high porosity limit case of a "multiple void process", i.e. a row of voids interacting and coalescing at the same time, for which the state of stress in the fracture process zone is almost uniaxial straining [1,2], the problem of Fig. 1 requires full numerical analysis of a crack tip blunting process coupled with a fracture process zone model. The present work follows previous computational studies pursued by several groups in France, Germany, U.K., Denmark, and in the U.S. (e.g. [3-10]), based on a continuum damage model implemented in a finite element code to simulate ductile tearing. One of the main problem encountered with this approach is the difficulty to properly introduce a length scale related to the spacing between defects within the constitutive model. The most simple way, but not the most rigorous, to introduce the length scale is to fix the element size along the crack path. This approach has been successful for simulating crack growth and, more specifically, for rationalizing constraint effects. However, the "material science point of view" of understanding the relationship between fracture toughness and microstructure is usually not much emphasized.

In this paper we explore trends in toughness in the case of 2D small scale yielding plane strain conditions. Two new aspects are introduced in the present analysis that have not been considered in previous modeling efforts devoted to linking the fracture toughness to the microstructure (e.g. [1,11-13]): (i) *void shape effects* (non-spherical voids ranging from penny-shape cracks to highly prolate voids are common in industrial metal alloys. Generally, forming processes also bring about a preferential orientation for the principal axis of the second phases and induce some degree of anisotropy in the void distribution. Furthermore, initially spherical void tends to elongate at low stress triaxiality and flattens at high stress triaxiality); (ii) A *micromechanically-based void coalescence model* involving the relative void spacing. This work also improves and extends former analyses which were based on a more approximate analysis of the coupling between damage and the crack tip state of stress [14].

The plan of the paper involves (i) a presentation of the model and of the computational methods; (ii) a critical assessment of the model towards recent calculations by Tvergaard and Hutchinson [2]; (iii) a synthesis of the main results of a generic 2D SSY study of the dependence of the fracture toughness on the flow and microstructural parameters of the models:

$$\frac{J_{Ic}}{\sigma_0 X_0} = F\left(\frac{\sigma_0}{E}, n, f_0, W_0, \lambda_0\right) \tag{1}$$

This section will also incorporate results dealing with the difference between the engineering toughness defined after a predetermined amount of crack growth and the physical toughness at the "true" cracking initiation.

VOID GROWTH MODEL AND COMPUTATIONAL METHODS

An enhanced model for void growth and coalescence. The extended Gurson model used in this paper to account for the effect of the growth and coalescence of voids on the behavior of the material has been presented in details in ref. [15-17]. It is based on the works by Gologanu *et al.* [18] for the account of the void aspect ratio and by Thomason [19] for the onset of coalescence with extensions to strain hardening and for the modeling of the coalescence process. The model is based on two different solutions for the growth of a void in an elastoplastic material, one solution is called "void growth" and corresponds to a regime of "diffuse" plasticity around the void and the other is called "void coalescence" and corresponds to localized plasticity in the intervoid ligament. These two solutions can be expressed under the form of two different plastic yield surfaces supplemented by evolution laws for the internal variables of the model (the porosity f, the void aspect ratio W, the relative void spacing, χ and the mean yield stress of the matrix material σ_y) and the normality rule for the plastic strain increment. The mode of plastic deformation changes from "void growth" to "void coalescence" when the yield surface intersects at the current loading point. These two yield surfaces are

$$\Phi_{growth} \equiv \frac{C}{\sigma_y^2}\left\|\boldsymbol{\Sigma}+\eta\Sigma_h\boldsymbol{X}\right\|^2 + 2q(g+1)(g+f)\cosh\left(\kappa\frac{\Sigma_h}{\sigma_y}\right) - (g+1)^2 - q^2(g+f)^2 = 0 \tag{2}$$

$$\Phi_{coalescence} \equiv \frac{\Sigma_e}{\sigma_m} + \frac{3}{2}\frac{|\Sigma_h|}{\sigma_m} - F(W,\chi) = 0 \tag{3}$$

The yield surface Φ_{growth} is the enhanced Gurson-type surface derived by Gologanu-Leblond-Devaux [18] and extended to strain hardening materials in ref. [15]. The yield function $\Phi_{coalescence}$ has been developed in the spirit of seminal work by Thomason, extended to the full coalescence response and to strain hardening. The symbol $\|\bullet\|$ represents the von Mises norm, $\boldsymbol{\Sigma}$ is the deviatoric stress tensor, Σ_h is a generalized hydrostatic stress, $\boldsymbol{X}$ is a "void rotation" tensor. Analytical

relationships link the dummy parameters C, η, g, κ, h_1, α_2 to the state variables W and f. The following uniaxial response has been chosen for the present study :

$$\frac{\sigma}{\sigma_0} = \frac{E\varepsilon}{\sigma_0} \quad \text{when } \sigma < \sigma_0, \tag{4a}$$

$$\frac{\sigma}{\sigma_0} = \left(1 + \frac{E\varepsilon^p}{\sigma_0}\right)^n \quad \text{when } \sigma > \sigma_0, \tag{4b}$$

Note finally that the model assumes that voids are present from the beginning of the loading and that the failure process ends by void impingement (i.e. no account is taken for other mechanisms such as local cleavage or second population of voids) that may accelerate coalescence.

A 2D small scale yielding analysis. The model described in the previous section has been implemented in the general purpose finite element code "ABAQUS Standard" through a User defined material subroutine (UMAT) with a fully implicit integration scheme [20]. An "infinite" cracked solid is modeled using a semi circular finite element mesh whose radius R is 10^7 times larger than the size of the representative element size in the fracture process region (see Fig. 2). Displacement rates corresponding to mode I plane strain K-field solution were prescribed on the outer boundaries while the crack surface is left traction free. A regular mesh with constant element size was designed in the near crack tip region. The crack tip is a round notch of diameter δ_0. In this paper, results will presented only for $\delta_0/X_0 = 0.1$ (i.e. a sharp initial crack simulating a fatigue precrack).

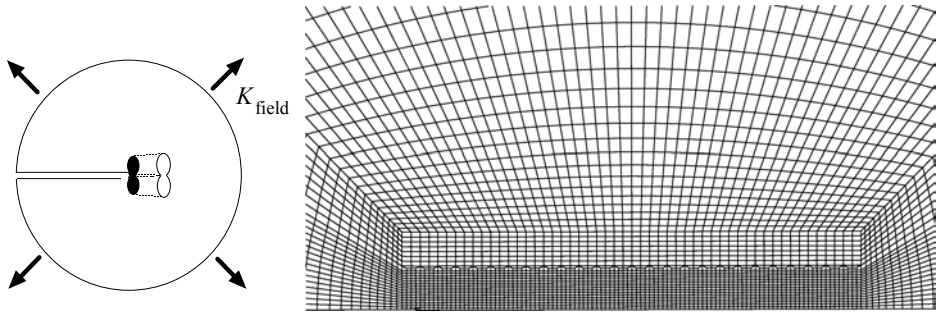

Figure 2: The 2D small scale yielding finite element model.

About the fracture length scale. The damage model used in this work has no length scale. To introduce a length scale, each element in the near tip region is viewed as a representative unit cell of length X_0 containing a single void (the damage model as been shown to adequately represent that situation when the cell is subjected to uniform displacements [15]). X_0 is the only length scale entering the analysis (when keeping the shape of the elements fixed for all calculations). All the results in this

paper will be normalized by X_0 which thus totally evacuates the dependence of the results on mesh refinement. Now, assimilating the element size to X_0 is obviously an approximation (because of the large strain gradients in fracture process zone) whose validity will be checked by the validation study described in the next section.

VALIDATION OF THE MODEL

In a recent report [2], Tvergaard and Hutchinson describe 2D SSY FE simulations of fracture initiation and tearing in J2 elastoplastic materials. A single row of cylindrical voids was explicitly introduced within the FE mesh as shown in Fig. 3. A fracture criterion is postulated for the final failure of the ligaments. Tractions in the ligaments are released for an imposed reduction, R, of the initial ligament length. Typically R was chosen equal to 1/2 or 1/3. That study offers a means to critically assess the model proposed in this paper. For that purpose, the failure criterion based on the reduction of ligament length was introduced in our model. The same parameters for the flow properties and initial microstructure have been used : σ_0/E = 0.003, n = 0.1, W_0 = 1, λ_0 = 1.

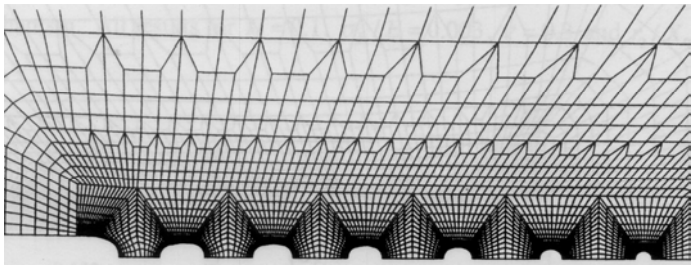

Figure 4. Finite element mesh used by Tvergaard and Hutchinson [2].

Fig. 4 compares the results for R = 1/2 and R = 1/3. The variations of $J_{Ic}/\sigma_0 X_0$ as a function of f_0 are very similar. The model predicts slightly larger normalized J. The good agreement between the two models means that the present model correctly capture the transition of failure mode described in [2] : at sufficiently high porosity, the void near the tip is influenced by its nearest neighbor, which experiences almost the same rate of growth. The interaction among the voids, including voids even farther from the tip, results in significantly higher rate of void growth for all of the voids. Coalescence between several voids and with the crack will start early and be almost simultaneous. This is the *multiple void interaction* mechanism. For sufficiently small void volume fraction, a single void process prevails, which is essentially the process modeled by Rice-Johnson [11]. The void nearest the tip grows with little influence from its nearest neighbor further from the tip. The increase of the normalized toughness with decreasing porosity is more marked. This is the *void by void growth* mechanism.

On Fig. 4 results have also been plotted for computations performed with damage in the entire material. The results are very similar to those obtained with one row of voids. However, we point out that during crack propagation the effect becomes significant: having voids on both sides of the fracture process zone tends to relax the stresses and to delay the localization, involving thus larger tearing resistance.

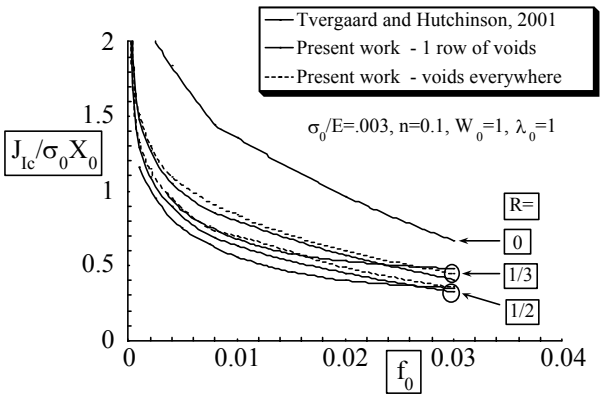

Figure 4: Variation of the fracture toughness as a function of the initial porosity, comparison with results by Tvergaard and Hutchinson [2].

Fig. 4 also shows results for R=0, i.e. final failure by impingement of voids with crack. The effect of R is important. The parameter R is strongly material dependent. In typical steel, second population of voids or micro-shear localization lead to premature ligament failure and values of R larger than 1/3 may be realistic. In other materials voids grow until final impingement with the crack. In this work, the value of R will be kept constant equal to 0. The results will thus give upper bound for the toughness of materials presenting some degree of "ligament embrittlement".

2D SSY PLANE STRAIN FRACTURE TOUGHNESS CALCULATIONS

Effect of the flow properties. Fig. 5a shows the effect of the ratio σ_0/E on $J_{Ic}/\sigma_0 X_0$ for n = 0.1. As expected from previous analyses [1] the toughness is proportional to the yield stress. Fig. 5b exhibits the effect of the strain-hardening capacity on the fracture toughness for a material with σ_0/E = 0.003, ν = 0.3, W_0 = 1, λ_0 = 1, and n = 0, 0.1 and 0.2. The strain hardening exponent is a very influent parameter.

The fact that the fracture toughness is proportional to the yield stress (Fig. 5a) seems to contradict many experimental evidences showing that the toughness usually decreases with increasing σ_0. First, in many materials, an increase of σ_0 is accompanied by a decrease of the strain-hardening capacity n. This is the case, for instance, in the age hardening of aluminum alloys (where precipitates responsible for the strengthening do not, in general, take part to the failure process and thus do not modify the initial void volume fraction). When comparing Fig. 5a and 5b, it

appears that the decrease of n can compensate or even dominate the effect on the toughness of an increasing yield stress. Secondly, the present model does not incorporate a damage nucleation stage. An increasing yield strength will affect the nucleation by raising the stress on the second phase particles or grain-boundary. Larger yield stress can also favor nucleation on smaller particles or on a second population of particles at an earlier stage of the deformation. However, it is clear that when all other parameters of the microstructure are kept constant, higher yield stress directly implies larger amount of energy spent in the fracture process zone to deform, damage and separate the material.

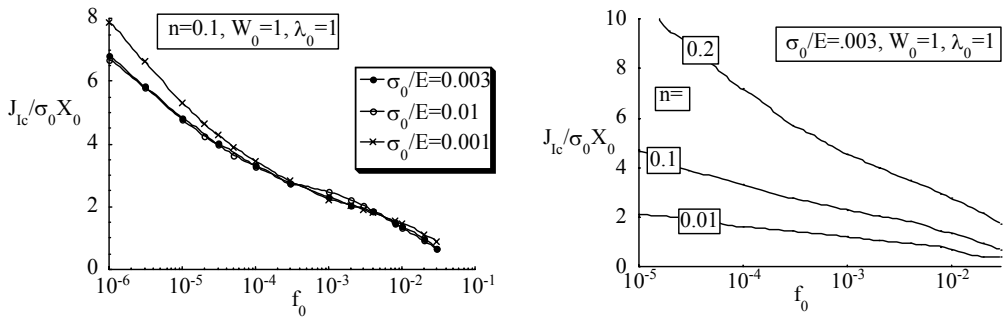

Figure 5: Variation of the fracture toughness as a function of the initial porosity for (a) different yield stress and (b) different strain-hardening exponent.

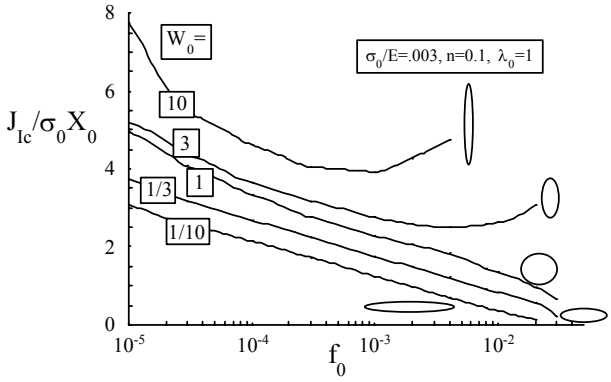

Figure 6: Effect of the initial void shape on the fracture toughness.

Void aspect ratio effect. Fig. 6 presents the variation of $J_{Ic}/\sigma_0 X_0$ as a function of f_0 for different initial void shapes ranging from $W_0 = 1/10$ (oblate) to $W_0 = 10$ (prolate), for $\sigma_0/E = 0.001$, $n = 0.1$, and $\lambda_0 = 1$. Prolateness tends to delay void coalescence by affecting the constraint in the ligament between the voids and also because, at a given porosity, a prolate shape implies larger void spacing. The results of Fig. 6 can

be used to address the variation of the fracture toughness as a function of the loading direction for rolled plates with preferential orientation of the second phase.

Physical versus engineering fracture toughness. The "engineering" definition of J_{Ic} implies that initiation is associated with a fraction of a millimeter or so of crack growth, which can amount to multiple void spacings for materials with closely spaced voids. The problem of the difference between the "first coalescence" estimate of the initiation toughness and the J_{Ic} defined on the basis of 0.2mm crack advance is depicted on Fig. 7 for two different materials with $f_0=10^{-3}$ and $f_0=10^{-4}$, showing the difference of toughness for materials with X_0=0.02mm or 0.2mm The difference between the true onset of cracking and the engineering definition in the case of materials with small X_0 (e.g. X_0=0.02mm in the example of Fig. 7) is not really an issue for structural integrity assessment but it is important when comparing the toughness of different materials.

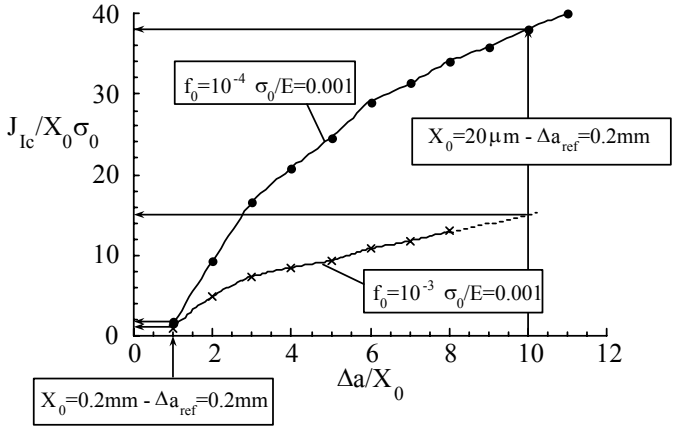

Figure 7: The difference between physical and engineering fracture toughness for two different materials with $f_0=10^{-3}$ or $f_0=10^{-4}$, considering X_0=0.02mm or 0.2mm

This consideration can, for instance, explain why experimental fracture toughness values may sometimes seem extremely large when looking at the void spacing X_0. For instance, Garrison and coworkers (e.g. [21] for a review) report many examples of high strength steels with inclusion spacings between 1 to 10 microns (σ_0/E in the range 0.001 range and f_0 in the range of 10^{-4}). The reported critical crack tip opening displacements are typically one to two orders of magnitude larger than the void spacing (i.e. $J_{Ic}/\sigma_0 X_0$=10 to 100). The reason is probably related to the fact that, for such small void spacing, the criterion given by the Standards to define initiation from a J_R-curve gives a value of J that involves plenty of void coalescence events. In that case, most of the energy involved in the engineering fracture toughness is related to extrinsic plastic dissipation. We also suspect that in

such materials constraint effects will affect the engineering fracture toughness when, for instance, changing the specimen configuration.

Acknowledgements

This work was carried out in the framework of the PAI 5-1-9 project "*From microstructure towards plastic behaviour of single- and multiphase materials*" supported by SSTC, Belgium.

References

1. Tvergaard, V., and Hutchinson, J.W., 1992. *J. Mech. Phys. Solids* 40, 1377-1397.
2. Tvergaard, V., and Hutchinson, J.W., 2001. Mech report 372, Harvard University.
3. Mudry, F., di Rienzo, F., and Pineau, A., 1989. In *Non-Linear Fracture Mechanics: Volume II - Elastic-Plastic Fracture*, ASTM STP 995 (Landes J.D., Saxena A. and Merkle J.G. eds.) ASTM, Philadelphia, 24-39.
4. Rousselier, G., Devaux, J.-C., Mottet, G., and Devesa, G., 1989. In *Nonlinear Fracture Mechanics: Volume II - Elastic-Plastic Fracture*, ASTM STP 995 (J.D. Landes, A. Saxena and J.G. Merkle eds.) ASTM, Philadelphia, 332-354.
5. Rivalin, F., Besson, J., Pineau, A., Di Fant, M., 2001. *Engng. Fract. Mech.* 68, 347-364.
6. Brocks, W., Klingbeil, D., Kunecke, G., and Sun, D.-Z., 1995a. In *Constraint Effects in Fracture Theory and Applications: Second Volume*, ASTM STP 1244 (Kirk M. and Bakker A. eds.) ASTM, Philadelphia, 232-252.
7. Bilby, B.A., Howard, I.C., and Li, Z.H., 1993. *Fatigue Fract. Engng. Mater. Struct.* 16, 1-20.
8. Needleman, A. and Tvergaard, V., 1987. *J. Mech. Phys. Solids* 35, 151-183.
9. Xia, L., Shih, C.F., and Hutchinson, J.W., 1995. *J. Mech. Phys. Solids* 43, 389-413.
10. Ruggieri, C., Panontin, T.L., and Dodds, R.H., Jr., 1996. *Int. J. Fract.* 82, 67-95.
11. Rice, J.R., and Johnson, M.A., 1970. In *Inelastic Behavior of Solids* (M. F. Kanninen, W. F. Adler, A. R. Rosenfield and R. I. Jaffee eds.) McGraw-Hill, 641-672.
12. Mudry, F., 1982. *Etude de la Rupture Ductile et de la Rupture par Clivage d'Aciers Faiblement Alliés*. Thèse d'état, Université de Technologie de Compiègne, France.
13. Ritchie, R.O., and Thompson, A.W., 1985. *Metall. Trans. A* 16, 233-248.
14. Pardoen, T. and Hutchinson, J.W., 2000. *Proceedings of the 13th European Conference on Fracture ECF13 - Fracture Mechanics: Applications and Challenges* (M. Fuentes *et al.* eds.) 6-9 Sep 2000, San Sebastian, Spain, CD-ROM Ref. 052c1.
15. Pardoen, T. and Hutchinson, J.W., 2000. *J. Mech. Phys. Solids* 48, 2467-2512.
16. Benzerga, A., 2000. *Rupture ductile de tôles anisotropes*. Ph. D. Thesis, Ecole Nationale Supérieure des Mines de Paris.
17. Pardoen, T. and Hutchinson, J.W. submitted to *Acta Materialia*.
18. Gologanu, M., Leblond, J.-B., Perrin, G., and Devaux, J., 1995. In *Continuum Micromechanics* (Edited by P. Suquet) Springer-Verlag.
19. Thomason, P.F., 1990. *Ductile Fracture of Metals*, Pergamon Press, Oxford.
20. ABAQUS 5.8, 1997. *User's Manual*, Hibbit, Karlsson & Sorensen, Providence, R.I., U.S.
21. Garrison, W.M., Jr., Wojcieszynski, and Iorio, L.E., 1997. In *Recent Advances in Fracture* (Mahidhara *et al.* eds.), TMS.